JOURNAL OF CATALYSIS 131, 573–581 (1991)

Mechanisms of the Formation of $PdNi_x$ in the Cages of NaY

JENNIFER S. FEELEY AND WOLFGANG M. H. SACHTLER

Center for Catalysis and Surface Science, Northwestern University, Evanston, Illinois 60208-3000

Received February 25, 1991; revised May 6, 1991

Three mechanisms by which Pd and Ni in the same zeolite enhance each other's reducibility and form bimetallic particles have been identified. Two series of bimetallic samples are compared with monometallic samples and their physical mixtures. In one series Pd^{2+} ions are initially positioned in sodalite cages, while NiO clusters occupy supercages. Upon reduction Pd atoms that leave the small cages are formed, and some become attached to NiO clusters and enhance their reduction. In the other series Ni^{2+} and Pd^{2+} ions are initially located in small cages. In this case two reduction mechanisms have been identified: below 200°C PdNi dimers are formed, which subsequently migrate to supercages; the activation energy for this migration is higher than that for Pd atoms. In a third mechanism unreduced Ni^{2+} ions start migrating at $T > 400$°C to Pd or $PdNi_x$ particles in supercages; subsequent reduction to $PdNi_x$ particles is fast. This process is reversible; at elevated temperature in an inert atmosphere the protons that were formed during reduction selectively reoxidize Ni atoms of $PdNi_x$ particles. Rereduction at $T > 400$°C reproduces the TPR peaks of the above process. The "leaching" of Ni atoms out of $PdNi_x$ particles is confirmed by the ability of the remaining Pd clusters to form Pd hydride.

I. INTRODUCTION

Previous results (*1–3*) on (Pd + Ni)/Na*X* and (Pt + Ni)/Na*X* samples showed an increase in both Ni reducibility and dispersion in the presence of Pd and Pt; however, no attempts were made in these early works to determine whether alloy formation occurred. More recently Pd (*4*) and Pt (*5, 6*) have been reported to enhance the reducibility of Ni supported on NaY zeolite. In particular, investigations in this lab explored the effects of washing at various pH values, calcination temperature (T_c) and Pd loading on this phenomenon using temperature-programmed reduction (TPR) (*4*).

The present study focuses on the formation of bimetallic "alloy" particles inside zeolite cages and dealloying by selective leaching of Ni. Temperature-programmed desorption is used to determine H_{ads}/Me^0 ratios, where Me^0 refers to the number of reduced metal atoms (Pd^0 + Ni^0). TPD was chosen over static chemisorption because TPD peak shifts relative to monometallic profiles can provide information on the formation of bimetallic particles.

The formation of bimetallic particles is also followed qualitatively by monitoring the presence or absence of hydride formation. Pd hydride is easily detected by a characteristic TPD peak; for bimetallic $PdNi_x$ particles such peaks are absent unless x and dispersion are both very low. Literature data (*7*) show that for $PdNi_x$, with $x > 0.2$, the solubility of hydrogen at 25°C and P_{H_2} = 1 atm is extremely low: $H/Me^0 < 0.05$. Under the same conditions the value is 0.7 for $x = 0$.

When applying TPD to determine the fraction of exposed metal atoms it is essential to realize that not all hydrogen released in a TPD is necessarily due to desorption of chemisorbed H atoms. Reoxidation of Ni by zeolitic protons has been quoted to cause a TPD peak at high temperature (*5, 6*). This reaction, Eq. (1), is the reverse of the reduction process:

$$Ni^0 + 2H^+ = Ni^{2+} + H_2. \qquad (1)$$

When applied to bimetallic particles this chemistry can lead to selective "leaching" of Ni out of PdNi particles. Leaching of Cu by zeolitic protons from bimetallic PtCu

0021-9517/91 $3.00

particles has been detected by EXAFS (*8*). Likewise, leaching of Cu from CuPd particles in (Cu + Pd)/NaY (*9*) has been detected by the ability of Cu-free Pd to form hydrides. This process is of considerable interest; its clarification for (Pd + Ni)/NaY forms one of the objectives of the present work. Identification of those TPD peaks that are due to Ni reoxidation rather than desorption of adsorbed hydrogen has been achieved by comparing TPD profiles with those of proton-free samples.

Previous results had clarified how metal-ion location and ligancy before reduction are controlled by calcination temperature (T_c) and pH (*10–16*). In the present work a T_c of 500°C was chosen in order to completely remove the ammine ligands of the Pd^{2+} ions and leave these ions predominantly in sodalite cages, irrespective of pH. Likewise the position of Ni^{2+} ions prior to reduction has been controlled by appropriate pretreatment conditions. It is known that after treatment at low pH Ni^{2+} ions migrate to the small cages during calcination (*4, 6, 12, 13, 17–19*), but after washing at high pH, small NiO clusters are formed in the supercages during calcination (*4, 10, 11*).

The particle growth mechanism for monometallic Pd/NaY samples, where Pd^{2+} ions occupy small cages before reduction, is well understood (*16, 20, 21*) and has been shown to occur in two steps. First, isolated Pd atoms, unable to dissociatively chemisorb H_2, are formed in sodalite cages. At higher reduction temperatures (T_r) these atoms escape from the small cages and form particles inside supercages. A maximum is obtained in the H_{ads}/Pd^0 ratio, as measured by H_2 TPD (*16*) and by the rate of benzene hydrogenation (*21*) at T_r of ca. 350°C. Higher T_r's result in particle agglomeration and concomitant loss in activity for this reaction.

It is of interest to verify whether analogous elementary steps can be identified in the particle growth mechanism for bimetallic zeolite-supported systems. This is accomplished in the present work by studying H_{ads}/Me^0 ratios as a function of T_r. Two scenarios will be compared: (A) (Pd + Ni)/NaY(A), where Pd^{2+} and Ni^{2+} ions both occupy small cages before reduction, and (B) (Pd + Ni)/NaY(B), where NiO clusters occupy supercages but Pd^{2+} ions are located in small cages.

II. EXPERIMENTAL

IIA. Sample Preparation

A series: Ni/NaY(A), Pd/NaY(A), and (Pd + Ni)/NaY(A). Linde LZ-Y52, NaY, was ion exchanged at a pH of 6.0 for 24 h at room temperature with either a 0.01 *M* $NiCl_2$ or $Pd(NH_3)_4(NO_3)_2$ solution for the monometallic samples. The bimetallic sample was prepared by a simultaneous exchange of the two metal ions. Following ion exchange, the samples were washed at a pH of 6.0 for 1 h using a dilute HNO_3 solution. The metal loadings in terms of number of atoms per unit cell, as determined by atomic absorption, were 8.8Ni for Ni/NaY(A), 10.0Pd for Pd/NaY(A), and 10.3Pd + 8.6Ni for (Pd + Ni)/NaY(A).

B series: Ni/NaY(B), Pd/NaY(B), and (Pd + Ni)/NaY(B). Ni/NaY, Pd/NaY, and (Pd + Ni)/NaY samples were washed at a pH of 10.5 using a dilute NaOH solution for 1 h following ion exchange to obtain B samples. Metal loadings were 8.8Ni for Ni/NaY(B), 10.0Pd for Pd/NaY(B), and 10.0Pd + 9.2Ni for (Pd + Ni)/NaY(B).

$(Pd + Ni)_{mix}$/NaY(A) and $(Pd + Ni)_{mix}$/NaY(B). These samples were prepared by physically mixing equal amounts of the corresponding monometallic samples described above.

$Ni/Pd_{red}/NaY(B)$. $NiCl_2$ was exchanged into Pd_{red}/NaY(B), described below, and then the sample was washed at a pH of 10.5. Metal loadings were 10.0 Pd and 8.8 Ni atoms per unit cell. Pd_{red}/NaY(B) was prepared by calcining Pd/NaY(B) in O_2 to 500°C for 2 h, followed by purging, and then reducing in H_2/Ar for 20 min at 350°C.

IIB. TPR/TPD Procedures

All temperature-programmed experiments were carried out *in situ* in a flow sys-

tem described previously (*14, 22*). Hydrogen consumption and evolution were monitored with a calibrated thermal conductivity detector (TCD). A molecular sieve trap, cooled to −78°C, was placed after the sample to trap any water formed during reduction. Catalysts, ca. 150 mg, were calcined in quartz microreactors in an O_2 flow of 180 ml/min from RT to 500°C at 0.5°C/min and then held at 500°C for 2 h. After calcination, samples were purged in Ar, 25 ml/min, at RT for 30 min and then cooled in Ar to −78°C, at which point the flow was switched to a mixture of 5% H_2/Ar, 25 ml/min. Samples were then reduced from −78°C to the specified reduction temperature, T_r, with a ramp of 8°C/min, and then held at T_r for 20 min. We refer to this treatment as TPR1. After TPR1, samples were cooled in the 5% H_2/Ar flow to RT, held there for 20 min, and then purged in Ar for 20 min at RT. This purging procedure has been shown to remove physisorbed H_2 and to decompose Pd hydride (*16, 23*). TPD profiles were then recorded in Ar, 25 ml/min, from −78°C to 760°C at 8°C/min. A second TPR, which we refer to as TPR2, was recorded immediately following TPD and cooling to −78°C in Ar. TPR2 was carried out with the same conditions as TPR1 with T_r = 760°C.

IIC. Calculation of H_{ads}/Me^0 Ratios

By comparing the areas of TPR1, TPD, and TPR2 with the weight loading of metal in the sample as determined by atomic absorption, it is possible to calculate H_{ads}/Me^0 values as well as the amount of Ni, if any, that is reoxidized during TPD. Recent results in this lab (*4*) have shown that H_2 consumption during TPR1, if carried out to 760°C, corresponds within 5% to the reduction of divalent Pd and Ni for all of the samples presented in this work. If no metal reoxidation occurs during TPD, the number of H_2 atoms consumed (TPR1 + TPR2) should correspond to the number of divalent metal ions present in the sample. This was found to be the case for all monometallic Pd samples as well as for the proton-free samples. For all other samples however, H_2/Me^{2+} ratios were consistently found to be in excess of 1.0 due to reoxidation of nickel during TPD. In addition, comparing the TPD areas to the TPR1 areas of these samples, without accounting for Ni reoxidation, often gave H_{ads}/Me^0 ratios that were significantly greater than 1.0. The extent of Ni reoxidation is thus determined by comparing the H_2 consumption in TPR1 + TPR2 with the known metal loading; the amount of chemisorbed hydrogen can then be calculated by subtracting H_2 evolution due to reoxidation from the total area of the TPD. All H_{ads}/Me^0 values in Table 1 have been determined in this manner and results were reproducible within 15% experimental error.

TABLE 1

Tr (°C)	%Ni reduced		%Ni reoxidized	
	A	B	A	B
200	20	23	—	—
300	48	31	17	5
400	54	56	31	32
500	60	60	25	31
600	82	77	44	45

Note. Tr, temperature of reduction after calcination to 500°C. A, (Pd + Ni)/NaY(A); B, (Pd + Ni)/NaY(B).

IID. Identification of Pd Hydride

Samples were subjected to one of two pretreatments, after T_c = 500°C, before probing for the Pd hydride phase. One treatment involved reduction at 600°C for 1 h and then cooling in H_2/Ar to −78°C; the other consisted of reduction at 600°C for 30 min followed by purging in Ar at 600°C for 30 min, cooling to RT in Ar and then switching to H_2/Ar and cooling to −78°C. Once at −78°C, all samples were subjected to a temperature-programmed hydride decomposition procedure which consisted of heating samples in a H_2/Ar flow of 25 ml/min to 100°C at 8°C/min. Hydrogen evolution, due

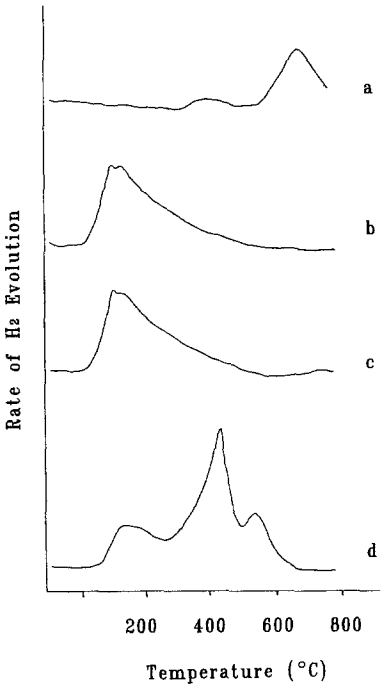

FIG. 1. TPD profiles of A Series: a) Ni/NaY(A) after Tr = 650°C; b) Pd/NaY(A) after Tr = 400°C; c) $(Pd + Ni)_{mix}$/NaY(A) after Tr = 400°C; d) (Pd + Ni)/NaY(A) after Tr = 400°C.

to decomposition of the Pd hydride phase, was monitored with a TCD cell and is evident as a negative peak in the TPD profile. Both monometallic Pd/NaY(A and B) and bimetallic (Pd + Ni)/NaY(A and B) samples were studied.

III. RESULTS

IIIA. TPD Results

A1. Monometallic samples. For Ni/NaY(A) a temperature program up to T_r = 650°C was required to reduce ca. 30% of the Ni. After this TPR1, the TPD profile shows two peaks (Fig. 1a), a small peak at ca. 400°C and a larger peak at ca. 650°C, similar to previous findings on comparable Ni/NaY samples (*5, 6*). The H_2/Ni^{2+} ratio determined by the sum of TPR1 and TPR2 was >1.0; the excess H_2 consumption corresponded to the area in the high-temperature TPD peak. This indicates that the H_2 evolution at high temperature is due to Ni reoxidation by protons (Eq. (1)). This hydrogen is therefore not included in the calculation of the H_{ads}/Me^0 ratio, which was found to be 0.08.

As found previously (*4, 10, 11*), Ni/NaY(B) was much easier to reduce than Ni/NaY(A). After T_r = 400°C, 32% of the Ni in Ni/NaY(B) was reduced. The TPD of Ni/NaY(B) after T_r = 400°C (Fig. 2a) shows one peak at ca. 400°C, which corresponded to H_{ads}/Me^0 of 0.15. Within 5% experimental error, the area of TPR2 corresponds to the reduction of the Ni that had not been reduced during the first TPR. No Ni reoxidation was detected during TPD for this proton-free sample.

The Pd/NaY(A) and Pd/NaY(B) samples were found to have TPR and TPD profiles virtually identical to those reported earlier for Pd/NaY samples, which were not subjected to any pH washes (*16*). In Figs. 1b

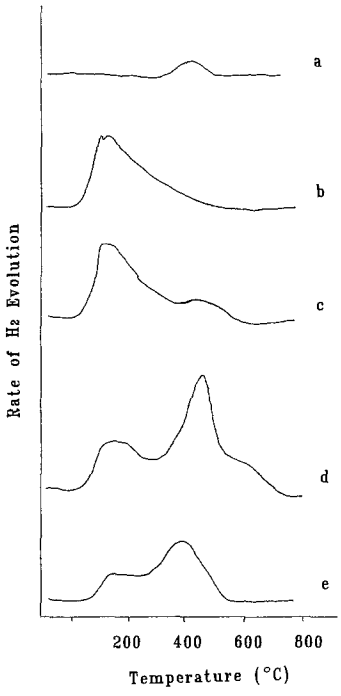

FIG. 2. TPD profiles of B Series after Tr = 400°C: a) Ni/NaY(B); b) Pd/NaY(B); c) $(Pd + Ni)_{mix}$/NaY(B); d) (Pd + Ni)/NaY(B); e) Ni/Pd_{red}/NaY(B).

and 2b the TPDs of Pd/NaY(A) and Pd/NaY(B) after T_r = 400°C are displayed, respectively. The H_{ads}/Me^0 ratios for these samples after T_r = 400°C are ca. 0.72. Reduction to 200°C in TPR1 results in complete reduction of Pd^{2+}; TPR2 profiles, carried out after TPD, show no further reduction, thus proving that no Pd reoxidation takes place during the TPD procedure.

A2. Physical mixtures and Ni/Pd_{red}/NaY(B). Figures 1 and 2 clearly show that the TPDs of the physical mixtures, (Pd + $Ni)_{mix}$/NaY(A) and (Pd + $Ni)_{mix}$/NaY(B), are simply linear combinations of those of the monometallic samples used in their preparation. This was previously found (*4*) to be the case for the TPR profiles of these samples. For (Pd + $Ni)_{mix}$/NaY(A), T_r = 400°C, no Ni is reduced and the TPD, Fig. 1c, is very similar to that of Pd/NaY(A), Fig. 1b. For (Pd + $Ni)_{mix}$/NaY(B), after T_r = 400°C, Ni reduction is ca. 30%, similar to Ni/NaY(B). In the TPD, Fig. 2c, no high-temperature Ni reoxidation peak is observed; the total H_2 consumption in TPR1 and TPR2 corresponds exclusively to the reduction of the divalent metals. This shows that no Ni reoxidation is observed when protons, although present, are not located in the same zeolite crystal as Ni^0.

For the proton-free bimetallic sample that was prepared by exchanging Ni^{2+} ions into Pd_{red}/NaY, followed by washing at high pH, no Ni reoxidation peak is observed in the TPD, Fig. 2e. Also, the sum of H_2 consumption in TPR1 + TPR2 corresponded exclusively to the reduction of the divalent metals. This confirms that the high-temperature peak present in the proton-containing bimetallic samples is due to reoxidation of Ni^0 by protons.

A3. Bimetallic samples. Table 1 lists the percentages of Ni in samples of the A and B series which are reduced during TPR1, and reoxidized during TPD as a function of T_r. It is clear that increasing T_r results in an increased amount of Ni reduction as reported earlier (*4*). In Fig. 3, H_{ads}/Me^0 ratios are plotted as a function of T_r for both of these series. The TPD profiles of (Pd + Ni)/NaY(A) and (Pd + Ni)/NaY(B), after T_r = 400°C, are presented in Figs. 1d and 2d, respectively.

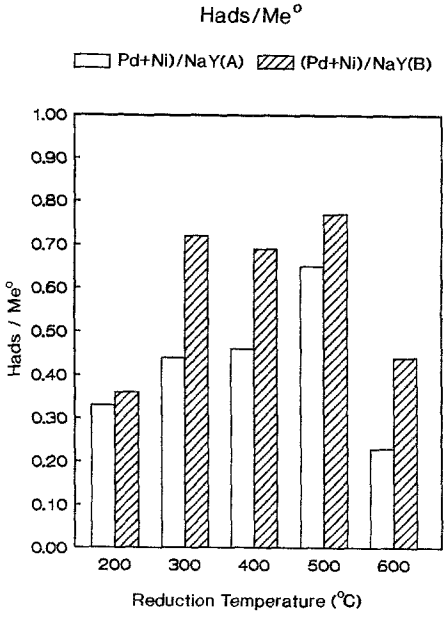

FIG. 3. H_{ads}/Me^0 Ratios for A and B series bimetallic samples as a function of Tr.

In both series, A and B, bimetallic samples exhibit an enhancement of Ni reducibility, which is not present in physical mixtures. For the A series, 54% of Ni is reduced in the bimetallic sample after T_r = 400°C, whereas no Ni reduction is observed under the same conditions for the corresponding physical mixture. In the B series, 56% of Ni is reduced in the bimetallic sample, after T_r = 400°C, compared to only 30% in the physical mixture. This enhanced reducibility results in H_{ads}/Me^0 ratios much higher than those for the monometallic Ni samples; i.e., for Ni/NaY(B) and (Pd + Ni)/NaY(B) after T_r = 400°C these ratios are 0.15 and 0.68, respectively.

The TPD profiles of bimetallic samples are strikingly different from those of monometallic samples or their physical mixtures, Figs. 1 and 2. This dramatic difference provides strong evidence for the formation of

bimetallic particles. In particular, the pronounced H_2 desorption peaks between 300 and 500°C, which dominate the TPD profiles of the bimetallic samples, are totally absent in the profiles of the physical mixtures. In addition, less H_2 desorption below 200°C is observed in the bimetallics. It is clear from these TPD results that the chemisorption properties of both metals, Pd and Ni, are significantly altered by the presence of the second metal in the same zeolite.

The presence of Pd also affects Ni reoxidation during TPD. In agreement with earlier findings for Ni/NaY and (Pt + Ni)/NaY samples (*5, 6*), the highest temperature peak in the TPD profiles appears to correspond roughly to the amount of Ni which is reoxidized. This Ni reoxidation peak is shifted to lower temperatures in the presence of Pd; i.e., compare Figs. 1a and 1d. A similar shift was found in the case of (Pt + Ni)/NaY (*5, 6*) and is construed as further evidence for the formation of bimetallic clusters.

The H_{ads}/Me^0 ratios in Fig. 3 are higher for the bimetallic B series than for the A series samples and the dependence of their ratios on T_r are quite different. In (Pd + Ni)/NaY(B), small NiO clusters occupy supercages (*4, 10, 11*) and Pd^{2+} ions are in the small cages (*14–16, 21*) before reduction. The dependence of the H_{ads}/Me^0 ratio, on T_r, for this sample is similar to that of monometallic Pd/NaY; i.e., the maximum H_{ads}/Me^0 is reached near T_r = 300°C (*16, 21*). The dispersion of (Pd + Ni)/NaY(B) at higher T_r's is, however, higher than that of Pd/NaY, i.e., H_{ads}/Me^0 = 0.78 vs 0.65 after T_r = 500°C (*16*). On the other hand, for (Pd + Ni)/NaY(A), where both Pd^{2+} and Ni^{2+} ions occupy small cages before reduction (*10, 12, 14–16, 18, 19*), maximum H_{ads}/Me^0 is reached only at T_r = 500°C.

IIIB. Pd Hydride Results

In Fig. 4a decomposition of Pd hydride is observed at ca. 25°C. This same TPD profile is observed for Pd/NaY(A) and Pd/NaY(B) after the pretreatments described in the experimental section. In contrast, no hydride is detected during TPD for the bimetallic samples, (Pd + Ni)/NaY(A and B), after reducing at 600°C and cooling in the reducing atmosphere (Fig. 4b). However, when these bimetallic samples were pretreated by reducing and then purging at 600°C, hydride decomposition is observed at ca. 15°C (Fig. 4c).

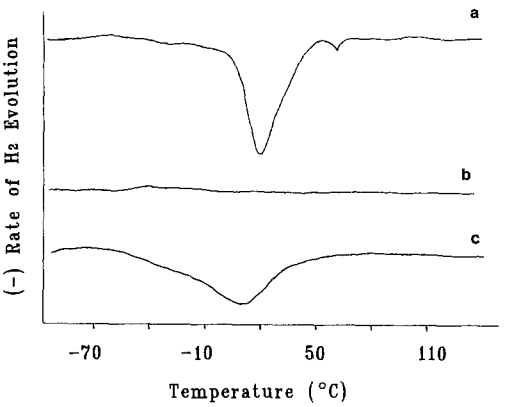

FIG. 4. Temperature Programmed Hydride Decompositions of a) Pd/NaY(A and B) after Tr = 600°C for 1 hr. or after Tr = 600°C for 30 min followed by purging in Ar at 600°C for 30 min; b) (Pd + Ni)/NaY(A and B) after Tr = 600°C for 1 hr.; c) (Pd + Ni)/NaY(A and B) after Tr = 600°C for 30 min followed by purging in Ar at 600°C for 30 min.

IIIC. TPR Results

In Fig. 5 the TPR1 and TPR2 profiles of (Pd + Ni)/NaY(A) are compared. The area of TPR1, carried out to 760°C, corresponds to the complete reduction of Ni^{2+} and Pd^{2+}. The first peak in this TPR is 40°C lower than the TPR peak of corresponding monometallic Pd sample indicating that Ni has enhanced the reducibility of Pd. TPR2 exclusively reflects the reduction of Ni^{2+} ions, which were formed by reoxidation of Ni^0 during the preceding TPD. Note that the position of the peaks above ca. 400°C are identical in these two TPRs.

IV. DISCUSSION

IVA. Evidence for Bimetallic Particle Formation

The additivity of the TPR and TPD profiles of physical mixtures and the strong de-

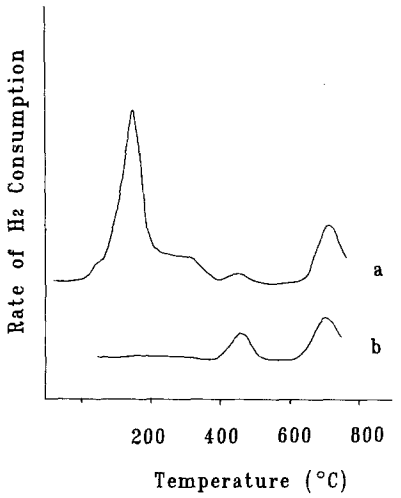

FIG. 5. Temperature Programmed Reduction Profiles of (Pd + Ni)/NaY(A): a) TPR1 [4]; b) TPR2.

viation from additivity of the profiles for the bimetallic samples that contain both metal precursors in the same zeolite crystal (Figs. 1 and 2) justify discussion of the latter observation in terms of an interaction between Pd and Ni. The TPD results indicate that the chemisorption properties of both Pd and Ni are significantly altered by the presence of the other metal, suggesting bimetallic particle formation.

It is well known that the presence of Ni in $PdNi_x$ alloys strongly inhibits the ability of Pd to *ab*sorb hydrogen (*7*). The striking lack of hydride formation in the bimetallic samples, in contrast to monometallic Pd/NaY, provides further evidence for the formation of $PdNi_x$ particles.

In agreement with previous findings for (Pd + Ni)/Na*X* samples (*1, 3*), significant enhancements in both Ni reducibility and dispersion were found in the present (Pd + Ni)/NaY samples. New information gained in the present work, however, indicates that bimetallic $PdNi_x$ particles are formed.

IVB. Mechanism of Enhanced Reduction

Significant enhancements in Ni reducibility and dispersion were found in both A and B series bimetallic samples with respect to the monometallic Ni analogs and physical mixtures. The primitive model for enhanced Ni reduction and particle growth, i.e., hydrogen spillover, cannot be reconciled with previous TPR results (*4*) or the current findings. The H_{ads}/Me^0 ratios of the A and B bimetallic series follow different trends with respect to T_r, reflecting the differences in the nature and location of Ni precursors before reduction. It is likely that different mechanisms control particle formation and growth for these two series.

The clearest situation is encountered for the bimetallic sample of the B series, (Pd + Ni)/NaY(B). In this sample only Pd^{2+} ions occupy the small cages (*14–16, 21*), while NiO clusters that are formed after calcination are located in the supercages (*4, 10, 11*). The maximum in H_{ads}/Me^0 for Pd/NaY and (Pd + Ni)/NaY(B) occurs at approximately the same T_r. It thus appears that the presence of NiO clusters in the supercages does not influence the reduction of Pd in the small cages and the migration of these atoms to supercages. Once reduced Pd atoms enter the supercages they can adhere to NiO clusters, which are then easily reduced due to dissociative chemisorption of H_2 on Pd. This reduction results in the formation of bimetallic particles. Although nucleation of Pd particles would also take place in those supercages that do not contain NiO clusters, leading to the formation of monometallic Pd particles as well as bimetallic $PdNi_x$ particles, the absence of Pd hydride shows that after reduction to 600°C, isolated Pd particles do not exist in significant numbers.

Several pathways for mutually enhanced reducibility are conceivable for the A series samples that contain, after calcination, both Pd^{2+} and Ni^{2+} ions in the small cages (*10, 12, 14–16, 18, 19*). One can imagine two mechanisms:

(1) Ni and Pd ions have some cation–cation interaction prior to reduction, which helps to dissociate H_2 and creates exothermic metal–metal bonds, resulting in PdNi dimers in the small cages.

(2) Pd is reduced first with no reduction enhancement by Ni. Ni^{2+} ions then migrate

to either (a) Pd atoms in the small cages or (b) Pd particles in the supercages, to be reduced.

The present data, in combination with previous results (*4*), are able to discriminate between these possibilities. Enhanced reducibility of Pd by Ni in the (Pd + Ni)/NaY(A) bimetallic sample, evidenced by a 40°C shift to lower temperature of the Pd TPR peak, was recently reported (*4*). This shift provides strong evidence for pathway (1) as one mechanism for the mutually enhanced reducibilities of Pd and Ni at low temperatures, i.e., below ca. 200°C. The presence of the resulting PdNi dimers and their retention in the small cages may explain why the maximum H_{ads}/Me^0 value is not reached until reduction to ca. 500°C.

The present study shows that pathway (2b) predominates at high temperatures, i.e., above ca. 400°C. The evidence is based on the comparison of profiles of TPR1 and TPR2 in Fig. 5. Curve 5b shows the reduction profile after virtually all of the Ni has been leached out of $PdNi_x$ particles by selective oxidation with zeolite protons. In this situation it can be fairly assumed that all Pd is present in the form of reduced Pd particles, whereas Ni is present as Ni^{2+} ions, most of which are located in the small cages. For the subsequent rereduction of this sample only mechanism (2b) is available. Therefore, we assign the two high-temperature peaks in curve 5b to two variants of this mechanism. This permits assignment of the same high-temperature peaks in curve 5b to the same mechanistic path. We therefore conclude that Ni reduction above 400°C is indicative for this path also in TPR1.

IVC. Leaching of Ni from PdNi Particles

Protons created during reduction conceivably reoxidize Ni^0 to Ni^{2+} at high temperature. Indeed, a "TPD peak" at high temperatures, ca. 400°C (Figs. 1d, 2d), which is absent in proton-free samples (Figs. 2a and 2e), demonstrates this reversal of the metal reduction process. Not surprisingly our results show that this process occurs only when protons and Ni^0 are located in the same zeolite crystal, as follows from comparison of Figs. 2c and 2d. The coreduction of Pd and Ni in bimetallic samples results in a proton concentration higher than that in monometallic Ni samples with the same Ni content, which may explain why this peak is shifted to lower temperatures in the former samples; compare Figs. 1a and 1d.

The selective reoxidation of Ni atoms from $PdNi_x$ particles corresponds to the electrochemical experience with bimetallic electrodes: in contact with a strong acid the less noble metal is selectively leached. As shown above, leaching of Ni from $PdNi_x$ particles is proven by formation of Pd hydride after leaching. This Pd hydride is unambiguously identified by its decomposition peak in Fig. 4c. The solubility curves of hydrogen in $PdNi_x$ alloys (*7*) show that significant hydride formation only occurs in alloy particles containing less than 20% Ni.

V. CONCLUSIONS

The formation of bimetallic $PdNi_x$ particles in (Pd + Ni)/NaY samples has been determined, by TPR, TPD, and by the absence of Pd hydride. Dealloying occurs by selective leaching of Ni from these bimetallic particles. After leaching of Ni, Pd hydride is observed. This Ni reoxidation occurs at high temperature under TPD conditions provided Ni^0 and protons occupy the same zeolite crystal.

The following mechanisms for bimetallic particle formation are operating depending on initial precursor locations:

(1) B Series: After calcination Pd^{2+} ions are located in small zeolite cages and NiO clusters occupy supercages. Pd^{2+} ions are reduced in the small cages followed by migration of Pd atoms to supercages where they adhere to NiO clusters, inducing an enhanced reducibility of NiO and formation of bimetallic particles.

(2) A Series: After calcination, both Pd^{2+}

and Ni^{2+} ions occupy small cages. Pd^{2+} and Ni^{2+} ions are coreduced in the small cages below ca. 200°C, resulting in a mutual enhancement in reducibility and PdNi dimer formation. At higher reduction temperatures, above ca. 400°C remaining Ni^{2+} ions migrate to supercages to be reduced in the presence of Pd and/or $PdNi_x$ particles, forming bimetallic particles.

ACKNOWLEDGMENTS

We gratefully acknowledge support from the U.S. Department of Energy, grant number DE-FGO2-87ERA3654 and the Mobil Foundation for a grant in aid. We also appreciate Dr. M. S. Tzou's stimulating ideas.

REFERENCES

1. Guilleux, M. F., Kermarec, M., and Delafosse, D., *J. Chem. Soc. Chem. Commun.*, 102 (1977).
2. Jeanjean, J., Delafosse, D., and Gallezot, P., *J. Phys. Chem.* **83**(21), 2761 (1979).
3. Guilleux, M. F., and Delafosse, D., *J. Chem. Soc. Faraday Trans. 1* **175,** 165 (1979).
4. Feeley, J. S., and Sachtler, W. M. H., *Zeolites* **10**(8), 738 (1990).
5. Jiang, H. J., Ph.D. thesis, Northwestern University, Evanston, IL, 1988.
6. Jiang, H. J., Tzou, M. S., and Sachtler, W. M. H., *React. Kinet. Catal. Lett.* **35,** 207 (1987).
7. F. A. Lewis, "The Palladium Hydrogen System," p. 85. Academic Press, London, 1967.
8. Tzou, M. S., Kusunoki, A. K., Kuroda, H., Moretti, G., and Sachtler, W. M. H., *J. Phys. Chem.*, in press.
9. Zhang, Z., Xu., L., and Sachtler, W. M. H., *J. Catal.*, in press.
10. Suzuki, M., Tsutsumi, K., Takahashi, H., and Saito, Y., *Zeolites* **8,** 284 (1988).
11. Sano, M., Maruo, T., Yamatera, H., Suzuki, M., and Saito, Y., *J. Am. Chem. Soc.* **109,** 52 (1987).
12. Gallezot, P., and Imelik, B., *J. Phys. Chem.* **77**(5), 652 (1973).
13. Thomas, J. M., and Williams, C. J., *Chem. Soc. Faraday Trans. 1* **84**(9), 2915 (1988).
14. Homeyer, S. T., and Sachtler, W. M. H., *J. Catal.* **117,** 91 (1989).
15. Gallezot, P., *Catal. Rev. Sci.* **20,** 121 (1979).
16. Homeyer, S. T., and Sachtler, W. M. H., *J. Catal.* **118,** 266 (1989).
17. Briend-Fraure, M., Jeanjean, J., Kermarec, M., and Delafosse, D., *J. Chem. Soc. Faraday Trans. 1* **74,** 1538 (1978).
18. Olson, D. H., *J. Phys. Chem.* **72**(13), 1538 (1968).
19. Dempsey, E., and Olson, D. H., *J. Phys. Chem.* **74**(2), 305 (1970).
20. Gallezot, P., and Imelik, B., *Adv. Chem. Ser.* **121,** 66 (1973).
21. Bergeret, G., Tri, T. M., and Gallezot, P., *J. Phys. Chem.* **87,** 1160 (1983).
22. Park, S. H., Tzou, M. S., and Sachtler, W. M. H., *Appl. Catal.* **24,** 85 (1986).
23. Boudart, M., and Hwang, H. S., *J. Catal.* **39,** 44 (1975).